colloids
and interfaces

MDPI

Article

Transport Behavior of Paranitroaniline through a Flat-Sheet Supported Liquid Membrane Using Tributylphosphate as a Carrier

Azizah Algreiby [1,*], Lama Alharbi [1], Noura Kouki [1], Haja Tar [1], Abrar Alnafisah [1] and Lotfi Béji [2]

[1] Department of Chemistry, College of Science, Qassim University, Buraydah 52571, Saudi Arabia; n.kouki@qu.edu.sa (N.K.)
[2] Department of Physics, College of Science, Qassim University, Buraydah 52571, Saudi Arabia
* Correspondence: grieby@qu.edu.sa; Tel.: +966-533-010-572

Abstract: 4-Nitroaniline (PNA) is a toxic organic compound commonly found in wastewater, posing significant environmental concerns due to its toxicity and potential carcinogenicity. In this study, the recovery of PNA from aqueous solutions was investigated using a supported liquid membrane (SLM). The membrane, which consists of polypropylene Celgard 2500 (PP-Celg), was embedded with the extractant tributyl phosphate (TBP). Various factors influencing the efficiency of PNA transportation were studied, including the concentration of PNA in the source phase, pH of the source phase, NaOH concentration in the receiving phase, and choice of stripping agents. Optimal conditions for the experiment were determined to be a source phase PNA concentration of 20 ppm at pH 7, distilled water as the receiving phase, TBP as the carrier in the organic phase, and a transport time of 8 h. The extraction process was conducted under ambient temperature and pressure conditions, yielding results indicative of a first-order linearized reaction. Additionally, membrane stability and liquid membrane loss were evaluated.

Keywords: 4-Nitroaniline (PNA); supported liquid membrane (SLM); polypropylene Celgard 2500 (PP-Celg); tributyl phosphate (TBP); separation

Citation: Algreiby, A.; Alharbi, L.; Kouki, N.; Tar, H.; Alnafisah, A.; Béji, L. Transport Behavior of Paranitroaniline through a Flat-Sheet Supported Liquid Membrane Using Tributylphosphate as a Carrier. *Colloids Interfaces* **2024**, *8*, 49. https://doi.org/10.3390/colloids8050049

Academic Editors: Ricardo Lopez Anton, Jose Maria De Teresa, Sion Federico Olive Méndez and Wuge Briscoe

Received: 9 July 2024
Revised: 22 August 2024
Accepted: 30 August 2024
Published: 4 September 2024

1. Introduction

PNA is an organic compound that is an intermediate in synthesizing pharmaceuticals, drugs, gasoline, and dyes. It is a solid powder with a bright yellow color and a slight ammonia-like odor. Due to its classification as a toxic compound particular handling, use, and disposal procedures must be in place for this substance [1,2]. It belongs to refractory pollutants commonly found in wastewater and, because of their toxicity and probable carcinogenic consequences, pose a serious threat to the environment.

The release of PNA during its production and utilization poses a serious environmental problem. It may cause long-term adverse effects in terms of hepatoxicity, splenotoxicity, and nephrotoxicity [3,4]. According to the United States Environmental Protection Agency (UEPA), this material is the top contaminant in water because of its toxicity, carcinogenicity, and mutagenicity. PNA metabolites are nonbiodegradable or slowly degradable and have varying toxicities to aquatic life and organisms. PNA is resistant to chemical and biological oxidation degradation due to a nitro group linked to the aromatic ring [5].

Treating wastewater containing PNA prevents environmental pollution and protects human health. Various methods have been developed for PNA removal. Wastewater containing PNA can be treated using physicochemical methods, such as adsorption, photodegradation, biodecomposition, and electrochemical treatment. Adsorption is the most effective method because it is easy to use, even when treating enormous amounts of wastewater. But adsorption methods for treating wastewater suffer from issues like high reagent consumption (e.g., adsorbents and catalysts) [6–8]. Also, a bioreactor widely used worldwide in methods for wastewater treatment is the biological aerated filter (BAF). Through carrier filtration and biodegradation, BAF can eliminate contaminants. BAF, a biofiltration-based wastewater treatment technique, has the features of high biomass retention, toxin tolerance, superior removal efficiency, and slurry separation [9,10]. However, bubble aeration in a BAF may lead to the stripping of volatile toxic and hazardous substances by air, resulting in secondary pollution [11]. The oxidation process (AOP), one of the technologies used in wastewater treatment, generates hydroxyl radicals (OH●), crucial oxidants in the breakdown of organic molecules. The final products of AOP include water, carbon dioxide, and various mineral ions, none of which are harmful to the environment. Despite having a high degrading capacity, AOP has drawbacks such as poor COD removal, poor stability, and expensive wastewater treatment in industrial applications. As a result, research has focused on creating novel techniques for treating water and wastewater to remove harmful industrial waste and organic chemicals [12–14].

Therefore, one alternative approach to existing wastewater treatment methods is the creation of cost-effective membranes that can adsorb PNA from aqueous solutions. Membrane processes are used as an environmentally friendly substitute to cleanse, separate, recover, or eliminate organic or inorganic components from liquid or gas media with minimal energy consumption, significantly reducing the waste volume without adding toxic compounds. The membrane technology is modular and able to work continuously. These processes apply to several economic sectors, such as the environment, energy, health, water treatment, cosmetics, food, and chemicals [15].

By using liquid membrane (LM) separation processes, a wide variety of organic and inorganic compounds can be effectively removed from aqueous solutions because of their simplicity in design, low energy costs, high selectivity, ease of operation, and ability to combine removal and recovery processes in one step. Heavy metals (although IUPAC recommends abandoning terms such as "heavy metals" [16]) are toxic environmental pollutants that accumulate in soil and water systems due to industrial discharges and agricultural runoff activities. Their presence poses significant health and environmental risks, necessitating effective recovery methods. Traditional approaches, such as chemical precipitation, coagulation, and ion exchange, often face challenges like high costs and sludge production. Advanced membrane technologies, including reverse osmosis and nanofiltration, offer improved efficiency but can be expensive and unstable.

Supported liquid membranes (SLMs) present a promising alternative due to their efficiency and cost effectiveness. SLMs require less solvent and fewer operational stages than traditional solvent extraction methods, leveraging high solute diffusion coefficients for better metal ion transport. Studies have demonstrated their effectiveness in recovering various metal ions (for example, metals belong to block d). For instance, research has shown that chelating oximes and solvating extractants like Cyanex 923 are effective for selective metal recovery. Additionally, supported ionic liquid membranes (SILMs) have been found to enhance selectivity and recovery efficiency. One study optimized SLM conditions for separating chromium (VI), copper, and zinc using D2EHPA as an extractant and acids as stripping reagents, focusing on parameters such as extraction duration and reagent concentrations. Another study developed a Fe (III) recovery model from spent alkaline batteries using Cyanex 923, highlighting SLM's economic advantages. Furthermore, SLM technology has proven effective in pre-concentrating trace metals from natural waters and detecting heavy metals like cadmium (Cd) in seawater, showcasing its versatility in environmental applications [17–20].

Among the membrane-based separation processes, León et al. used an emulsion liquid membrane process to remove PNA from aqueous solutions. This optimized the removal process by analyzing the efficiency of PNA removal from the feed phase and the initial apparent feed/membrane fluxes and permeabilities under various experiments [21]. In addition, Tao et al. simultaneously performed a two-/three-phase hollow fiber-based liquid-phase micro-extraction (HF-LPME) method for the determination of aromatic amines in environmental water samples, including PNA.

All liquid membranes consist of an extractant agent (carrier) in an organic solvent that selectively binds to one or a class of components in the aqueous feed phase and transports it to the aqueous receiving phase through the membrane [22]. The carrier needs to be highly selective and very specific to the solution that needs to be eliminated. The most widely utilized carriers include hydro-oximes, amines, crown ethers, and phosphoorganic molecules. Carriers are mainly divided into three classes based on their functional groups: acidic, basic, and neutral:

i. Acidic Carriers: they are the most efficient at extracting the cations, as the carriers do form complex salt with cations with the exchange of protons. The acidic carriers contain COOH, P (OH), SO_3H, or chelating groups. ii. Basic Carriers: The anionic metal complexes are extracted using the alkaline/basic carriers. The best examples of such carriers are amines. iii. Neutral Carriers: For the purpose of selectively transporting various metal ions in LMs, neutral carriers are typically employed as cation carriers. They carry the metal ions in their cavities. The extraction efficiency of such neutral carriers depends on the size of their cavity and the size of the inserted ions. An anion and a cation are transported across the LM simultaneously when these carriers are employed as metal ion carriers in the membrane phase. The most common neutral carriers in LM processes are macrocyclic molecules and organic phosphoryl compounds. Tributylphosphate is a refractory molecule that is particularly difficult to degrade. Kumbasar used the separation method using emulsion liquid membranes and using TBP as an extractant. TBP is a neutral extractant. To preserve electrical neutrality, neutral extractants frequently extract cations or uncharged metal complexes together with the associated anions. Most of the neutral extractants that have been investigated in the liquid membrane studies are organophosphoryl compounds, including trioctylphosphine oxide (TOPO), TBP, and tributhylphosphine oxide (TBPO) [23–25].

TBP is the most widely used phosphatic solvent due to its high extraction selectivity [26]. It is usually used as an extractant to separate metal ions with good extraction efficiency [27]. Liu et al. used mixed carriers containing trioctylmethylammonium chloride (Aliquat 336) and TBP and used poly (vinyl) chloride (PVC) as the base polymer for the recovery of phenolic compounds from aqueous solutions [28]. The transfer of Nb (V) and Ta (V) ions in a chloride medium across a supported liquid membrane containing TBP as a carrier has been investigated [29]. Synergistic reactive extraction of platinum (IV) from aqueous solution was conducted using an organic phase consisting of TBP and bis (2, 4, 4-trimethylpentyl monothiophosphinic acid (Cyanex 302) in kerosene [30].

In this investigation, we will develop an SLM for removing an aromatic compound PNA from an aqueous solution using TBP as an extractant. An attempt has been made to optimize this technique's process parameters to obtain an efficient separation system.

2. Materials and Methods

2.1. Materials

PNA (MERCK-Schuchardt, Switzerland, ≥99%) was dissolved in ultrapure water (Milli Q Plus Colum, Millipore, Burlington, MA, USA) to create the feed solutions (Table 1).

All chemicals used were of analytical reagent grade. NaOH (CDH, New Delhi, India, 97%), NaCl (Pacegrove, Leicestershire, UK, 99%), and sodium acetate (Loba Chemie, Mumbai, India, 99%) were used as strippants.

Table 1. Chemical formula, molecular weight, and chemical structure of 4-nitroaniline.

4-Nitroaniline	**(MERCK-Schuchardt)**
Chemical formula	$C_6H_6N_2O_2$
Molecular weight	138.12 g mol^{-1}
Chemical structure	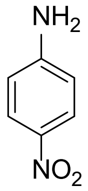

2.1.1. Polymeric Support

Polypropylene (Celgard 2500, Celgard Inc., Charlotte, NC, USA) was used as a polymeric support for the organic solution (Table 2).

Table 2. Physical characteristics of polymeric support.

Thickness d_0 (µm)	**Pore Diameter d (µm)**	**Porosity ε (%)**	**Tortuosity ($\tau = 1 - \ln\varepsilon$)**
25	0.064	55	1.598

2.1.2. Extractant

The polymeric support was impregnated using TBP as a carrier. Table 3 gives the chemical formula, molecular weight, and chemical structure of TBP.

Table 3. Chemical formula, molecular weight, and chemical structure of TBP.

Tributyl Phosphate	**(Fluka Chemika, 99%)**
Chemical formula	$(C_4H_9)_3PO_4$
Molecular weight	266.32 g mol^{-1}
Chemical structure	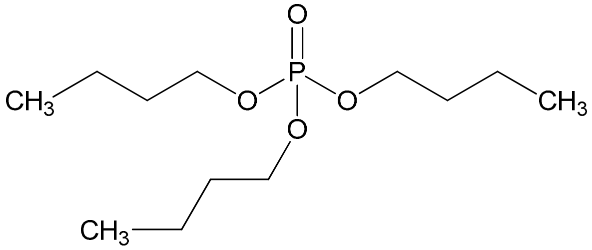

2.2. Membrane Preparation

Experiments on PNA extraction were performed at about 25 °C in a permeation cell. The organic liquid consisting of TBP was saturated in the membrane for 24 h, a crucial step ensuring the membrane was fully prepared for extraction. By weighing the polymeric support before and after immobilization, we determined the amount of TBP that was immobilized. An additional layer of carrier was removed by wiping it with a soft piece of paper. The obtained SLM was fixed between the two half-cells of the device, with an exposed membrane area of 3.14 cm^2. Source and receiving solutions (50 mL each) were placed into two compartments on the device and mixed using two magnetic stirrers. For both aqueous feeding and stripping solutions, magnetic stirring at 600 rpm at 25 °C avoided concentration polarization at membrane interfaces and in bulk solutions. The schematic illustration of the SLM process is shown in Figure 1. Using a pipette, 0.5 mL of the source and receiving solutions were removed hourly during the transport operation and diluted to a suitable volume. After that, these solutions were examined at a wavelength of 379 (Shimadzu UV–visible spectrophotometer 1650, Kyoto, Japan), and a calibration curve was used to determine the concentration of the PNA in each sample.

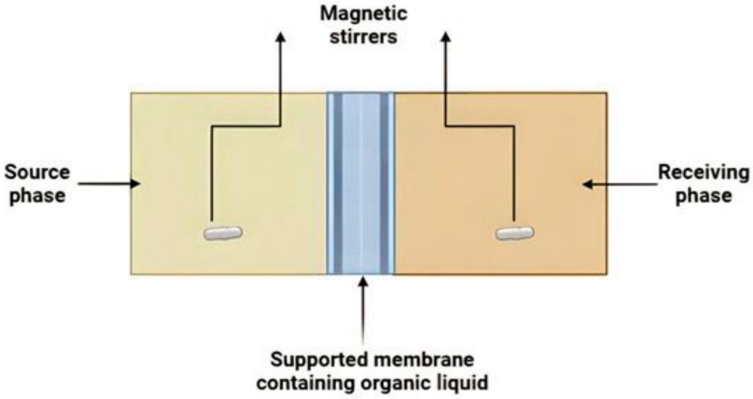

Figure 1. Schematic diagram of SLM process.

The E and R (%) were calculated using the following equation:

$$E\% = \frac{[\text{PNA}]_{\text{donor},0} - [\text{PNA}]_{\text{donor},t}}{[\text{PNA}]_{\text{donor},0}} \times 100 \quad (1)$$

$$R\% = \frac{[\text{PNA}]_{\text{receiving},t}}{[\text{PNA}]_{\text{donor},0}} \times 100 \quad (2)$$

where $[\text{PNA}]_{\text{donor},0}$ is the concentration of PNA in the initial source solution, $[\text{PNA}]_{\text{donor},t}$ is the concentration of PNA in the source solution after transport, and $[\text{PNA}]_{\text{receiving},t}$ is the concentration of PNA in the receiving phase after transport.

2.3. Buffer Solution Preparation

Table 4 describes the preparation methods of the two buffers used in this study.

Table 4. Methods for preparing buffer.

Buffer pH = 4	**Buffer pH = 12**
The buffer solution (pH = 4) is prepared by mixing a solution of succinic acid 0.2 mol L^{-1} (V = 25 mL) and a solution of NaOH 0.2 mol L^{-1} (10 mL). Ultrapure water was added to the mixture to obtain a 100 mL solution.	The buffer solution (pH = 12) is prepared by mixing a solution of glycine 0.2 mol L^{-1} (V = 25 mL) and a solution of NaOH 0.2 mol L^{-1} (23.35 mL). Ultrapure water was added to the mixture to obtain a 100 mL solution.

3. Results and Discussion

3.1. Transport of PNA with and without Carrier

The variation in E (%) and R (%) during the 8 h of transport is shown in Figure 2. The presence of the carrier (TBP) in the polymeric support leads to a noticeable improvement in the transport of the PNA from the feed to the receiving phase. The E (%) and the R (%) increase from 6.743 to 68.169 and from 3.053 to 49.2226, respectively, with and without impregnation. Moreover, after 8 h, the transport stops and the E (%) and R (%) remain constant. This behavior could be related to the carrier's loss from the membrane. There is a possibility that carrier losses are related to its solubility (solubility of TBP in water is 0.4 g L^{-1} at 25 °C), as membrane liquid (ML) is not completely insoluble in an aqueous solution and some solubility exists at the ML/aqueous solution interface. This influence can be significant if ML is highly soluble in nearby aqueous solutions [31,32]. In their study of TBP-mediated transport of phenol, Huidong et al. showed that emulsion formation was responsible for membrane instability [33]. Based on the thickness $d_{0,A}$, porosity ϵ_A, and tortuosity τ_A of Accurel® PP support, the experimental (J_{exp}) and normalized (J_N) fluxes for

PNA were calculated (J_{exp} = 7 × 10^{-10} and J_N = 0.51 × 10^{-10} mol m^{-2} s^{-1}) using Celgard 2500 [24,34].

$$J_N = J_{exp} \frac{d_0 \tau}{\epsilon} \frac{\epsilon_A}{d_{0,A}\, \tau_A} \tag{3}$$

where d_0, τ, and ϵ represent the membrane thickness, tortuosity, and porosity, respectively.

$$J_{exp} = \left(\frac{V}{A}\right)\left(\frac{dC}{dt}\right) \tag{4}$$

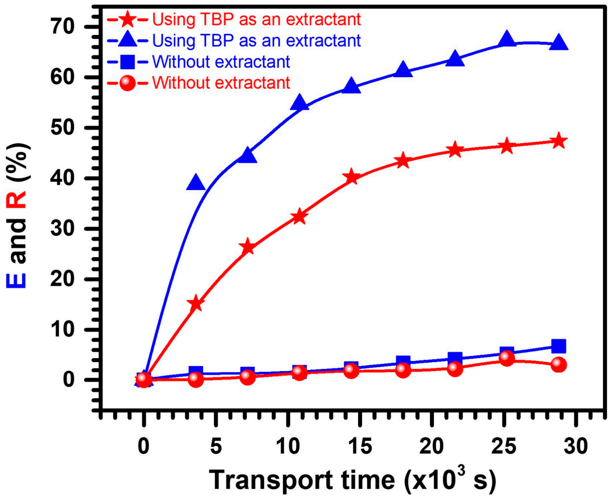

Figure 2. Variation in the E and R (%) as a function of the transport time. Feed solution: PNA 20 ppm; receiving solution: distilled water; membrane phase: PP-Celg without TBP and with TBP as extractant.

The receiving phase volume (L), the active area of the membrane (m^2), the concentration of PNA (mol L^{-1}), and the transport time (s) are represented by V, A, C, and t, respectively. The slope $\frac{dC}{dt}$ is determined by the linear variation in the PNA concentration over time in the receiving phase.

The effect of UV radiation on transport efficiency was investigated (Table 5). Firstly, the polymeric support was irradiated with UV radiation for 15 min and 180 min, and after that, it was impregnated with TBP. The obtained system was used as a membrane phase. After 8 h of transport, the R (%) percentages were calculated and found to be 47.72% and 44.61%, respectively, for 15 and 180 min of irradiation. Therefore, the R (%) values indicate that the irradiation of the membrane with UV radiation does not affect the transport efficiency.

Table 5. Variation in the E and R (%) as a function of the transport time. Feed solution: PNA 20 ppm; receiving solution: distilled water; membrane phase: PP-Celg without TBP and with TBP as extractant.

Time of Irradiation (min)	R (%)
0	46.59
15	47.72
180	44.61

3.2. Liquid Membrane Loss

The weight of the wet and used membrane supports was measured to calculate the LM loss, and they were represented as m_{wet} and m_{used}, respectively (see Figure 3). The wet membrane indicates the polymeric support after impregnation. Following the removal, the utilized membrane was obtained. It was dried in a silica gel vessel until its mass was stable. The LM phase loss per unit area was then calculated using the following equation Δm (%) [35,36]:

$$\begin{aligned} \text{LM phase loss, } \Delta m\ (\%) &= \frac{m_{wet}-m_{used}}{m_{wet}} \times 100 \\ \Delta m(\%) &= \frac{0.0293-0.0127}{0.0293} \times 100 \\ \Delta m &= 56.655 \end{aligned} \tag{5}$$

where m_{wet} and m_{used} are the weights of the wet and used polymeric supports, respectively.

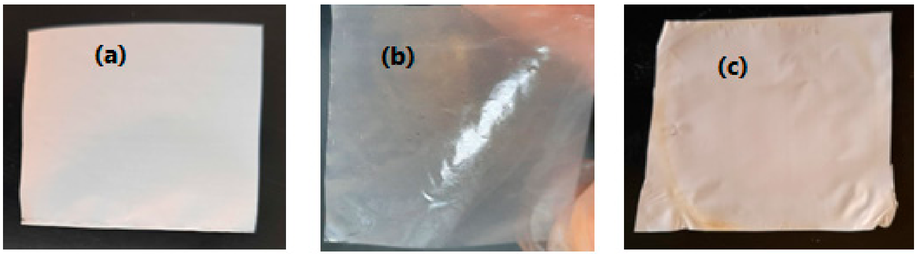

Figure 3. Real photos of PP-Celg membrane: (**a**) membrane before impregnation; (**b**) m_{wet}; (**c**) m_{used}.

To mitigate the leaching of TBP, we propose future studies exploring the use of other types of polymeric support, the use of alternative carriers with lower environmental impact, the addition of electrolytes in the aqueous phases, the addition of surfactants in the LM, and the application of a polymeric gel layer on the outer surface of SLM to reduce the emulsion formation. These steps aim to enhance the sustainability and industrial applicability of the SLM system.

3.3. Effect of PNA and NaOH Concentration

The percentage of PNA removal by varying initial feed phase concentration from 20 to 80 ppm is shown in Figure 4a. The removal performance was not influenced by an increase in PNA concentration. The E and R (%) are around 48.8 and 46.5%, respectively. In fact, TBP is not adequate carrier to transport PNA proportionally. It can be also attributed to carrier saturation and the smaller effective membrane area because of concentration boundary layer formation on the interface between the feed and membrane phases, which cause PNA to remain in feed phase and, accordingly, PNA pertraction remains constant at higher concentrations. Moreover, solution ionic strength at higher concentrations is more important. This also causes a lower PNA activity coefficient and hence reduces PNA activity to form complexes [37–40].

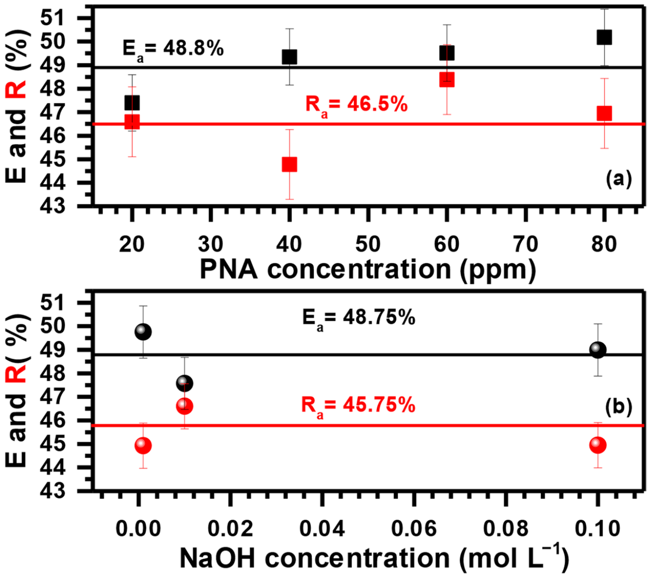

Figure 4. Variation in the E and R (%) as a function of the concentration of the PNA phase source (**a**) and (**b**) the concentration of the NaOH receiving solution at a transport time equal to 8 h.

Figure 4b illustrates the removal efficiency of PNA by varying the concentration of the stripping agent. It is clear from Figure 4b that the increase in the NaOH in the stripping phase has no impact on the transport efficiency. The E and R (%) are around 48.75% and 45.75%, respectively. Therefore, the transport of PNA from the organic-phase–receiving-phase interface occurs without any counter ion.

3.4. Selection of Stripping Agents

The receiving phase and its concentration play an important role in deciding the final recovery of the target solute by the SLM process. However, very few reports are available on the effect of stripping agents on the performance of the SLM process [41]. In this study, various stripping agents like NaOH, CH_3COONa, and NaCl were used as the receiving phase to evaluate the performance of SLM. Therefore, to achieve complete transport of PNA and avoid its back transport, we have selected a 0.01 mol L^{-1} concentration of each stripping. The feed was kept constant at 20 ppm of PNA (pH 7), the PP polymer was impregnated with TBP, and the run time was 8 h. The E and R (%) are (47.3966, 46.59), (55.391, 50.209), (51.079, 48.201), and (50.36, 49.015) for H_2O, NaCl, NaOH, and CH_3COONa, respectively (Figure 5). The results indicated a slight E (%) increase when NaCl is used as a stripping agent. This slight increase could be explained by a better affinity to the counter ion Cl^- than OH^- and CH_3COO^- [42].

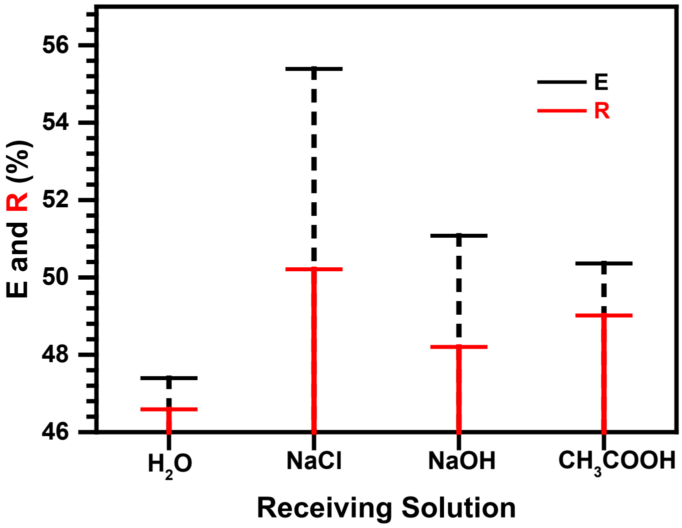

Figure 5. The effect of the strippants' nature on E and R (%). Feed solution: PNA 20 ppm; receiving solution: (H_2O, NaCl 0.01 mol L^{-1}, NaOH 0.01 mol L^{-1}, CH_3COONa 0.01 mol L^{-1}); organic phase: TBP; membrane (PP-Celg).

3.5. Effect of the Initial pH of the Source Phase

The effect of pH on PNA removal efficiency is shown in Figure 6. The R (%) values are 46.33, 46.59, and 46.46% for pH = 4, pH = 7, and pH = 12, respectively. The obtained values are almost equal. Hence, the initial pH of the donor phase did not influence the transport of PNA through the membrane.

At pH < 7, 4-nitroaniline would react with the H_3O^+ ions in the medium to give its conjugated acid:

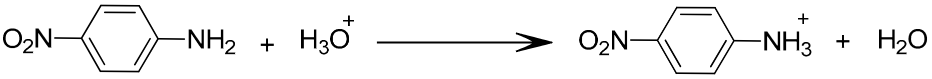

The potential interaction between PNA and TBP could involve non-covalent interactions, such as hydrogen bonding or van der Waals forces, rather than traditional coordination bonds in metal complexes. PNA from the aqueous phase (aq) interacts with TBP in the organic phase (org) to form a complex in the organic phase. It is important to note that providing a detailed and accurate representation of the complex formation is easier with specific experimental data or computational studies. The interactions between organic compounds like PNA and solvents like TBP can vary widely, and the actual behavior would need to be determined through experimental investigations or theoretical studies tailored to the specific system of interest.

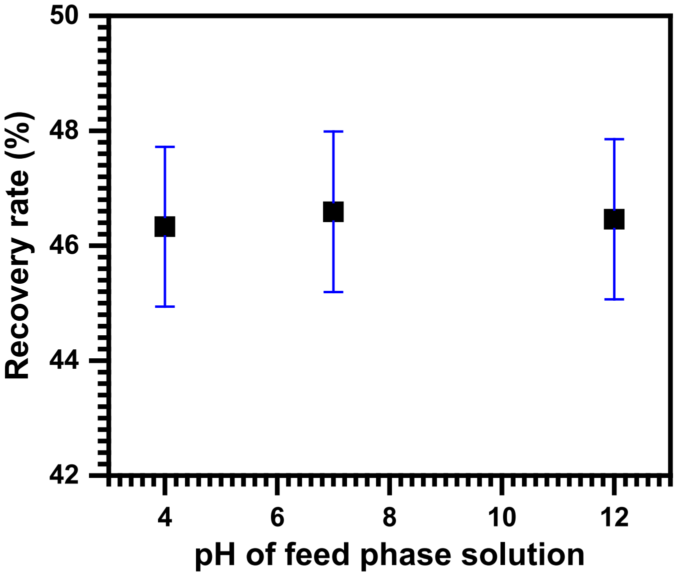

Figure 6. Variation in E and R (%). Feed solution: PNA 20 ppm at different pH (pH = 4, pH = 7, and pH = 12); receiving solution: distilled water; organic phase: TBP; membrane: PP-Celg.

The mechanism of transport can be summarized in three steps [43–45]:

Step 1: Formation of a complex between PNA and TBP via hydrogen bond at the first interface feed phase-membrane;
Step 2: Migration of the formed complex through the membrane;
Step 3: Formation of a complex between water existing in the receiving phase and release of the PNA in the receiving phase.

$$[\mathrm{PNA}]_{aq} + [\mathrm{TBP}]_{org} \rightleftarrows [\mathrm{PNA.TBP}]_{org} \tag{6}$$

$$[\mathrm{PNA.TBP}]_{org} + [\mathrm{H_2O}] \rightleftarrows [\mathrm{TBP.H_2O}]_{org} + \mathrm{PNA} \tag{7}$$

3.6. Membrane Stability

The reusability of the membrane was studied in two manners. Firstly, the stability of the membrane support was carried out by repeatedly using the same membrane support without further impregnation with the liquid membrane. Experimental conditions are as follows: feed phase PNA 20 ppm (pH 7), strip phase distilled water, TBP as carrier, and transport time 8 h. Fresh feed and strip solutions are used in every cycle. A total of 1 mL of each solution is taken after 8 h to find their concentrations. The R (%) calculations during four successive cycles demonstrate that the membrane is unstable. The R (%) decreases significantly from 46.59 to 5.7% for the first and last cycles. This instability could be attributed to the saturation of the membrane with PNA, slow stripping, and marginal leaching of TBP. Secondly, membrane stability was developed by re-impregnating the polymeric support with TBP after each cycle. The same experimental conditions are taken into consideration. Figure 7 reveals that the R (%) remains almost constant. Therefore, re-impregnating the membrane after each cycle improves the performance of the elaborated system. Also, this improvement confirms that the loss of the carrier is one of the reasons causing the system instability.

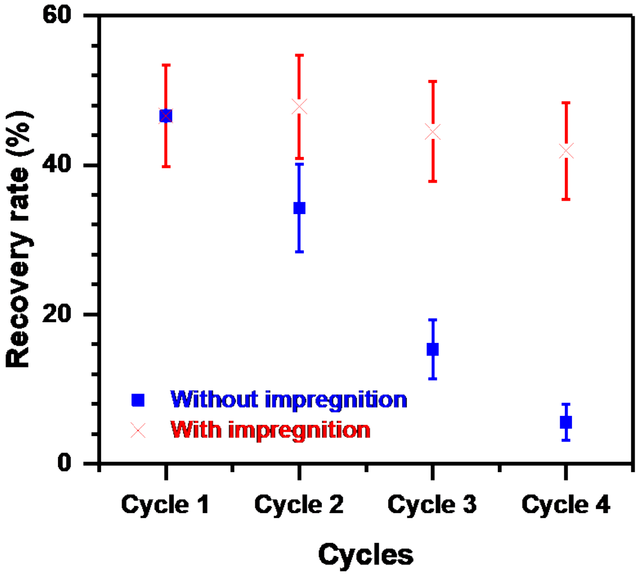

Figure 7. Variation in the E and R (%) per cycle. Feed solution: PNA 20 ppm; Receiving solution: distilled water; Organic phase: TBP; Membrane: PP-Celg; Cycle duration: 8 h.

3.7. Extraction Kinetics

Supported liquid membrane (SLM) transport studies were carried out by extracting PNA under ideal circumstances, 20 ppm (pH 7) of source phase concentration, distilled water in the receiving phase, carrier TBP as the organic phaser, and a duration of 8 h. PNA was extracted at room temperature and atmospheric pressure. Samples from the feed phase were taken every hour and analyzed using UV spectrophotometry. The evaluation of the PNA extraction kinetics under the operational conditions was estimated by fitting the time-course performance data with the first-order linearized reaction by the following equation [46,47]:

$$\mathrm{Ln}\,\frac{C_t}{C_0} = -K_a\,t \tag{8}$$

where $[\mathrm{PNA}]_{\mathrm{donor,t}}$ the feed phase concentration at time t, $[\mathrm{PNA}]_{\mathrm{donor,0}}$ is the initial feed phase, and K_a is the apparent rate constant. A plot of ln C_t/C_0 versus time shows a straight line having a slope of 5.28 × 10^{-5} (Figure 8). Hence, the extraction of PNA using SLM follows first-order kinetics with the apparent rate constant $K_a = 5.28 \times 10^{-5}\ \mathrm{s}^{-1}$.

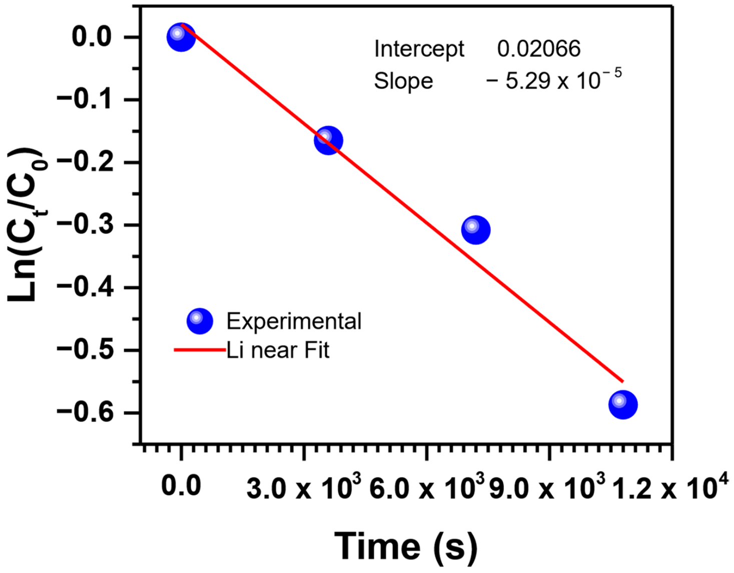

Figure 8. First-order plot for extraction of PNA.

4. Conclusions

In conclusion, this study elucidates the potential of supported liquid membrane (SLM) technology for the removal of 4-Nitroaniline (PNA) from aqueous solutions, addressing the pressing environmental concerns posed by this toxic compound. Through systematic experimentation and optimization, we identified key factors influencing the transportation efficiency of PNA, including source phase concentration, pH, choice of carrier, and stripping agents. Our results demonstrate that under optimal conditions, the extraction and re-extraction percentages are around 50%. The developed system exhibits first-order linearized reaction kinetics.

Furthermore, the stability of the membrane and the extent of liquid membrane loss were evaluated, shedding light on practical considerations for the implementation of SLM systems in real-world applications. While membrane stability proved to be a challenge, particularly in terms of carrier leaching and saturation, strategies such as re-impregnation of the membrane with tributyl phosphate (TBP) after each cycle showed promise in improving system performance.

Author Contributions: Methodology, N.K.; validation, N.K.; formal analysis, H.T. and A.A. (Abrar Alnafisah); investigation, A.A. (Azizah Algreiby) and L.B.; writing—original draft, L.A.; writing—review and editing, A.A. (Azizah Algreiby) and N.K.; supervision, A.A. (Azizah Algreiby) and N.K. All authors have read and agreed to the published version of the manuscript.

Funding: The Researchers would like to thank the Deanship of Graduate Studies and Scientific Research at Qassim University for financial support (QU-APC-2024-9/1).

Data Availability Statement: The original contributions presented in the study are included in the article; further inquiries can be directed to the corresponding author.

Conflicts of Interest: The authors declare no conflicts of interest.

References

1. Trivedi, M.K.; Branton, A.; Trivedi, D.; Nayak, G.; Bairwa, K.; Jana, S. Impact of biofield treatment on spectroscopic and physicochemical properties of p-nitroaniline. *Insights Anal. Electrochem.* **2015**, *1*, 1–8. [CrossRef]
2. Zhao, Y.S.; Sun, C.; Sun, J.Q.; Zhou, R. Kinetic modeling and efficiency of sulfate radical-based oxidation to remove p-nitroaniline from wastewater by persulfate/Fe_3O_4 nanoparticles process. *Sep. Purif. Technol.* **2015**, *142*, 182–188. [CrossRef]
3. Jayachandrabal, B.; Tikker, P.; Preis, S. Oxidation of aqueous p-Nitroaniline by pulsed corona discharge. *Sep. Purif. Technol.* **2022**, *297*, 121473. [CrossRef]
4. Mahmoud, M.E.; Abdou, A.E.; Shehata, A.K.; Header, H.M.; Hamed, E.A. Behavior of γ-Al_2O_3-bonded-3-chloropropyltrimethoxysilane nanosorbent toward potential binding and removal of 4-nitroaniline and 2-amino-3-nitro-pyridine from water. *J. Mol. Liq.* **2016**, *224*, 1358–1369. [CrossRef]
5. Malakootian, M.; Gharaghani, M.A.; Dehdarirad, A.; Khatami, M.; Ahmadian, M.; Heidari, M.R.; Mahdizadeh, H. ZnO nanoparticles immobilized on the surface of stones to study the removal efficiency of 4-nitroaniline by the hybrid advanced oxidation process (UV/ZnO/O_3). *J. Mol. Struct.* **2018**, *1176*, 766–776. [CrossRef]
6. Liou, T.-H.; Huang, J.-J. Efficient Removal of Hazardous P Nitroaniline from Wastewater by Using Surface-Activated and Modified Multiwalled Carbon Nanotubes with Mesostructure. *Toxics* **2024**, *12*, 88. [CrossRef]
7. Liu, J.; Li, Y.; Li, K. Optimization of preparation of microporous activated carbon with high surface area from Spartina alterniflora and its p-nitroaniline adsorption characteristics. *J. Environ. Chem. Eng.* **2013**, *1*, 389–397. [CrossRef]
8. Ali, N.S.; Harharah, H.N.; Salih, I.K.; Saady, N.M.C.; Zendehboudi, S.; Albayati, T.M. Applying MCM-48 mesoporous material, equilibrium, isotherm, and mechanism for the effective adsorption of 4-nitroaniline from wastewater. *Sci. Rep.* **2023**, *13*, 9837. [CrossRef]
9. Bao, T.; Chen, T.; Wille, M.-L.; Ahmadi, N.E.; Rathnayake, S.I.; Chen, D.; Frost, R. Synthesis, application and evaluation of non-sintered zeolite porous filter (ZPF) as novel filter media in biological aerated filters (BAFs). *J. Environ. Chem. Eng.* **2016**, *4*, 3374–3384. [CrossRef]
10. Farabegoli, G.; Chiavola, A.; Rolle, E. The Biological Aerated Filter (BAF) as alternative treatment for domestic sewage. Optimization of plant performance. *J. Hazard. Mater.* **2009**, *171*, 1126–1132. [CrossRef]
11. Mei, X.; Ding, Y.; Wang, Y.; Yang, Y.; Xu, L.; Wang, Y.; Shen, W.; Zhang, Z.; Ma, M.; Guo, Z.; et al. A novel membrane-aerated biofilter for the enhanced treatment of nitroaniline wastewater: Nitroaniline biodegradation performance and its influencing factors. *Bioresour. Technol.* **2020**, *307*, 123241. [CrossRef] [PubMed]
12. Malakootian, M.; Pournamdari, M.; Asadipour, A.; Mahdizadeh, H. Degradation and removal of p-nitroaniline from aqueous solutions using a novel semi-fluid Fe/charcoal micro-electrolysis reactor. *Korean J. Chem. Eng.* **2019**, *36*, 217–225. [CrossRef]

13. Sun, J.-H.; Sun, S.-P.; Fan, M.-H.; Guo, H.-Q.; Qiao, L.-P.; Sun, R.-X. A kinetic study on the degradation of p-nitroaniline by Fenton oxidation process. *J. Hazard. Mater.* **2007**, *148*, 172–177. [CrossRef] [PubMed]
14. Mohamed, R.M.; Aazam, E.S. Photocatalytic conversion of 4-nitroaniline to p-phenylenediamine using Ni/ZnSn$(OH)_6$ nanoparticles. *J. Ind. Eng. Chem.* **2014**, *20*, 3329–3334. [CrossRef]
15. Eljaddi, T.; Laurent, L.; Miloudi, H. Review on mechanism of facilitated transport on liquid membranes. *J. Membr. Sci. Res.* **2017**, *3*, 199–208. [CrossRef]
16. Duffus, J.H. "Heavy Metals"—A Meaningless Term? *Pure Appl. Chem.* **2002**, *74*, 793–807. [CrossRef]
17. Goh, S.S.; Rafatullah, M.; Ismail, N.; Alam, M.; Siddiqui, M.R.; Seow, E.-K. Separation of chromium (VI), copper and zinc: Chemistry of transport of metal ions across supported liquid membrane. *Membranes* **2022**, *12*, 685. [CrossRef]
18. Sarfraz, S.; Abid, A.J.; Javed, M.; Iqbal, S.; Aljazzar, S.O.; Zahra, M.; Alrbyawi, H.; Elkaeed, E.B.; Somaily, H.H.; Pashameah, R.A.; et al. Chromium (III) Ions Were Extracted from Wastewater Effluent Using a Synergistic Green Membrane with a BinaryCombination of D2EHPA and Kerosene. *Catalysts* **2022**, *12*, 1220. [CrossRef]
19. Alguacil, F.J.; Lopez, F.A. Separation iron (III)-manganese (II) via supported liquid membrane technology in the treatment of spent alkaline batteries. *Membranes* **2021**, *11*, 991. [CrossRef]
20. Pont, N.; Salvadó, V.; Fontàs, C. Applicability of a supported liquid membrane in the enrichment and determination of cadmium from complex aqueous samples. *Membranes* **2018**, *8*, 21. [CrossRef]
21. León, G.; Hidalgo, A.M.; Gómez, M.; Gómez, E.; Miguel, B. Efficiency, Kinetics and Mechanism of 4-Nitroaniline Removal from Aqueous Solutions by Emulsion Liquid Membranes Using Type 1 Facilitated Transport. *Membranes* **2024**, *14*, 13. [CrossRef] [PubMed]
22. Farah, M.; Giralt, J.; Stüber, F.; Font, J.; Fabregat, A.; Fortuny, A. Supported liquid membranes for the removal of pharmaceuticals from aqueous solutions. *J. Water Process. Eng.* **2022**, *49*, 103170. [CrossRef]
23. Ghoshal, A.K.; Saha, P. Liquid–membrane filters. In *Progress in Filtration and Separation*; Academic Press: Cambridge, MA, USA, 2015; pp. 155–205. [CrossRef]
24. Sastre, A.M.; Kumar, A.; Shukla, J.P.; Singh, R.K. Improved techniques in liquid membrane separations: An overview. *Sep. Purif. Methods* **1998**, *27*, 213–298. [CrossRef]
25. Rzelewska-Piekut, M.; Regel-Rosocka, M. Liquid membranes for separation of metal ions from wastewaters. *Phys. Sci. Rev.* **2021**, *8*, 937–982. [CrossRef]
26. Zhou, Z.; Fan, J.; Liu, X.; Hu, Y.; Wei, X.; Hu, Y.; Wang, W.; Ren, Z. Recovery of lithium from salt-lake brines using solvent extraction with TBP as extractant and $FeCl_3$ as co-extraction agent. *Hydrometallurgy* **2020**, *191*, 105244. [CrossRef]
27. Hu, Z.; Zhang, T.; Lv, L.; Chen, Y.; Zhong, B.; Tang, S. Extraction performance and mechanism of TBP in the separation of Fe^{3+} from wet-processing phosphoric acid. *Sep. Purif. Technol.* **2021**, *272*, 118822. [CrossRef]
28. Liu, Y.; Xie, H.; Qin, Z.; Lu, L.; Wang, L.; Sun, L.; Gu, Y.; Zhang, Y. Synergism induced intensification for the recovery of phenolic compounds using polymer inclusion membranes containing binary mixed carriers. *J. Environ. Chem. Eng.* **2024**, *12*, 112981. [CrossRef]
29. Campderrós, M.E.; Marchese, J. Facilitated transport of niobium(V) and tantalum (V) with supported liquid membrane using TBP as carrier. *J. Memb. Sci.* **2000**, *164*, 205–210. [CrossRef]
30. Sulaiman, R.N.R.; Othman, N.; Jusoh, N.; Noah, N.F.M.; Rashid, R.; Saufi, S.M. Intensification reactive recovery of tetravalent platinum from spent catalyst via synergism of TBP/Cyanex 302 system. *Chem. Eng. Process.* **2021**, *168*, 108581. [CrossRef]
31. Danesi, P.R.; Reichley, L.; Rickert, P.G. Lifetime of supported liquid membranes: The influence of interfacial properties, chemical composition and water transport on the long term stability of the membranes. *J. Membr. Sci.* **1987**, *31*, 117–145. [CrossRef]
32. Chiarizia, R. Stability of SLMs containing long-chain aliphatic amines as carriers. *J. Membr. Sci.* **1991**, *55*, 65–77. [CrossRef]
33. Zheng, H.; Wang, B.; Wu, Y.; Ren, Q. Instability Mechanisms of Supported Liquid Membrane for Phenol Transport. *Chin. J. Chem. Eng.* **2009**, *17*, 750–755. [CrossRef]
34. Stolwijk, T.B.; Sudhoelter, E.J.R.; Reinhoudt, D.N. Crown Ether Mediated Transport: A Kinetic Study of Potassium Perchlorate Transport through a Supported Liquid Membrane Containing Dibenzo-18-Crown-6. *J. Am. Chem. Soc.* **1987**, *109*, 7042–7047. [CrossRef]
35. Sulaiman, R.N.R.; Jusoh, N.; Othman, N.; Noah, N.F.M.; Rosly, M.B.; Rahman, H.A. Supported liquid membrane extraction of nickel using stable composite SPEEK/PVDF support impregnated with a sustainable liquid membrane. *J. Hazard. Mater.* **2019**, *380*, 120895. [CrossRef]
36. Zhao, W.; He, G.; Nie, F.; Zhang, L.; Feng, H.; Liu, H. Membrane liquid loss mechanism of Supported ionic liquid membrane for gas separation. *J. Membr. Sci.* **2012**, *411–412*, 73–80. [CrossRef]
37. Mahdavi, H.R.; Arzani, M.; Isanejad, M.; Mohammadi, T. Effect of hydrophobic and hydrophilic nanoparticles loaded in D2EHPA/M2EHPA—PTFE supported liquid membrane for simultaneous cationic dyes pertraction. *J. Environ. Manag.* **2018**, *213*, 288–296. [CrossRef]
38. Kazemi, P.; Peydayesh, M.; Bandegi, A.; Mohammadi, T.; Bakhtiari, O. Pertraction of methylene blue using a mixture of D2EHPA/M2EHPA and sesame oil as a liquid membrane. *Chem. Pap.* **2013**, *67*, 722–729. [CrossRef]
39. Madaeni, S.; Jamali, Z.; Islami, N. Highly efficient and selective transport of methylene blue through a bulk liquid membrane containing Cyanex 301 as carrier. *Sep. Purif. Technol.* **2011**, *81*, 116–123. [CrossRef]

40. Muthuraman, G.; Palanivelu, K. Transport of textile dye in vegetable oils based supported liquid membrane. *Dye Pigment.* **2006**, *70*, 99–104. [CrossRef]
41. Pilli, S.R.; Banerjee, T.; Mohanty, K. 1-Butyl-2,3-dimethylimidazolium hexafluorophosphate as a green solvent for the extraction of endosulfan from aqueous solution using supported liquid membrane. *Chem. Eng. J.* **2014**, *257*, 56–65. [CrossRef]
42. Bhosale, V.K.; Chana, H.K.; Kamble, S.P.; Kulkarni, P.S. Separation of nitroaromatics from wastewater by using supported ionic liquid membranes. *J. Water Process. Eng.* **2019**, *32*, 100925. [CrossRef]
43. Kumar, A.; Manna, M.S.; Ghoshal, A.K.; Saha, P. Study of the supported liquid membrane for the estimation of the synergistic effects of influential parameters on its stability. *J. Environ. Chem. Eng.* **2016**, *4*, 943–949. [CrossRef]
44. Naganawa, H.; Tachimori, S. Highly Hydrated Associate of Tributyl Phosphate in Dodecane. *Anal. Sci.* **1994**, *10*, 607–613. [CrossRef]
45. Srirachat, W.; Usapein, P.; Kheawhom, S.; Pancharoen, U. Selective separation of trace nickel(II) and gold(I) ions via hollow fiber supported liquid membrane enhanced by synergistic extractants D2EHPA/TBP. *Arab. J. Chem.* **2021**, *14*, 103427. [CrossRef]
46. Parham, H.; Saeed, S. Ultrasound-assisted solid phase extraction of nitro- and chloro-(phenols) using magnetic iron oxide nanoparticles and Aliquat 336 ionic liquid. *J. Chromatogr. A* **2014**, *1336*, 34–42. [CrossRef]
47. Kazemi, P.; Peydayesh, M.; Bandegi, A.; Mohammadi, T.; Bakhtiari, O. Stability and extraction study of phenolic wastewater treatment by supported liquid membrane using tributyl phosphate and sesame oil as liquid membrane. *Chem. Eng. Res. Des.* **2014**, *92*, 375–383. [CrossRef]